[28] C. J. Brabec, S. E. Shaheen, C. Winder, N. S. Sariciftci, P. Denk, *Appl. Phys. Lett.* **2002**, *80*, 1288.
[29] P. Peumans, S. R. Forrest, *Appl. Phys. Lett.* **2001**, *79*, 126.
[30] P. Peumans, S. R. Forrest, *Chem. Phys. Lett.* **2004**, *398*, 27.
[31] P. Maslak, A. Chopra, *J. Am. Chem. Soc.* **1993**, *115*, 9331.
[32] C.-L. Lin, H.-W. Lin, C.-C. Wu, *Appl. Phys. Lett.* **2005**, *87*, 021 101.
[33] A. Rapp, C. Bock, H. Dittmar, K. O. Greulich, *J. Photochem. Photobiol., B* **2000**, *56*, 109.
[34] T. P. I. Saragi, R. Pudzich, T. Fuhrmann, J. Salbeck, *Appl. Phys. Lett.* **2004**, *84*, 2334.
[35] Y.-Y. Noh, D.-Y. Kim, Y. Yoshida, K. Yase, B.-J. Jung, E. Lim, H.-K. Shim, *Appl. Phys. Lett.* **2005**, *86*, 043 501.
[36] K.-S. Narayan, N. Kumar, *Appl. Phys. Lett.* **2001**, *79*, 1891.

Highly Efficient, Deep-Blue Doped Organic Light-Emitting Devices**

By *Meng-Ting Lee*, *Chi-Hung Liao*, *Chih-Hung Tsai*, and *Chin H. Chen**

In recent years, there has been considerable interest in developing blue organic light-emitting devices (OLEDs) with high efficiency, deep-blue color, and long operational lifetime. The deep-blue color is defined arbitrarily as having blue electroluminescent (EL) emission with a Commission Internationale de l'Eclairage *y* coordinate value (CIE_y) of < 0.15. Such emitters can effectively reduce the power consumption of a full-color OLED and can also be utilized to generate light of other colors by energy cascade to a suitable emissive dopant.

It is well known that a guest–host doped emitter system can significantly improve device performance in terms of EL efficiency and emissive color, as well as operational lifetime.[1] Although many blue host materials have been reported, such as anthracene,[2] di(styryl)arylene,[3] tetra(phenyl)pyrene,[4] terfluorenes,[5] and tetra(phenyl)silyl derivatives,[6] blue-doped emitter systems having *all* the attributes of high EL efficiency, long operational lifetime, and deep-blue color, are rare.[7] This is because designing a fluorescent, deep-blue dopant capable of forming an amorphous glassy state upon thermal evaporation with a much shortened π-conjugation length is a rather daunting task. In addition, finding a deep-blue dopant with a small Stokes shift is essential for efficient Förster energy transfer from the host to dopant molecules, since the energy transfer efficiency is highly dependent on the spectral overlap between the emission of the host and the absorption of the dopant.

Recently, we have successfully demonstrated an anthracene-based blue host material, 2-methyl-9,10-di(2-naphthyl)-anthracene (MADN), which possesses a wide energy bandgap of 3.0 eV and can also form a stable thin-film morphology upon thermal evaporation. When doped with a di(styryl)-amine-based blue dopant, *p*-bis(*p*-*N*,*N*-diphenyl-aminostyryl)-benzene (DSA-Ph), it achieved a very high EL efficiency of 9.7 cd A^{-1}, with a greenish-blue color of $CIE_{x,y}$ (0.16, 0.32) and a long operational lifetime of 46 000 h at a normalized initial brightness of 100 cd m^{-2}.[8] However, the color saturation of the blue-doped emitter system (DSA-Ph@MADN) is far from adequate for application in full-color OLED displays. On the other hand, the symmetrical di(styryl)amine-based organic molecule is well known to possess a high fluorescent quantum yield,[9] and its emission wavelength (λ_{max} = 450–480 nm) is dependent on the π-conjugation length, which encompasses the two strongly donating arylamine moieties. However, the molecular engineering of symmetrical di(styryl)amine-based fluorescent dyes to cause hypsochromic shift has its limitations as both donors are already present as part of the styryl π-conjugation.[10]

In this paper, we report a series of novel, deep-blue dopants based on unsymmetrical mono(styryl)amine derivatives, which provide us with a basic structure for color tuning within the 430–450 nm spectral region. We show that when doped in the MADN host as an OLED, some of these deep-blue dopants exhibit all the essential elements of high EL efficiency, deep-blue color, and long operational lifetime. We find also that the EL efficiency of the device can be further improved by employing a hole-blocking layer (HBL) or a novel composite hole-transport layer (c-HTL) in the conventional blue OLED architecture.

The mono(styryl)amine-based deep-blue dopants used for this study are readily synthesized by the Horner–Wadsworth–Emmons reaction according to a known procedure,[9] and the molecular structures are shown in Scheme 1. By modifying the substituents attached to the nitrogen (R_1 and R_2) as well as to the styrene (R_3), it is possible to optimize the structure to achieve various desirable emissions in the deeper blue region of the visible spectrum. This is exemplified by the solution photoluminescence (PL) of **BD1**, **BD2**, and **BD3** in toluene as compared with DSA-Ph in Figure 1. Their peak fluorescence λ_{max} are located at 438, 442, and 448 nm, and their full width at half maximum (FWHM) values are 58, 62, and 64 nm, respectively, which is about 20 nm smaller than that of the sky-blue dopant, DSA-Ph (λ_{max} = 458 nm, FWHM = 58 nm). The hypsochromic shift is believed to result from shortening the chromophoric conjugation as well as modifying of the aromatic substituents of the mono(styryl)amine-based dopants.

[*] Prof. C. H. Chen
Display Institute, Microelectronics and Information Systems Research Center
National Chiao Tung University
Hsinchu, Taiwan 300 (Taiwan)
E-mail: fredchen@mail.nctu.edu.tw
Dr. M.-T. Lee, C.-H. Liao, C.-H. Tsai
Department of Applied Chemistry
National Chiao Tung University
Hsinchu, Taiwan 300 (Taiwan)

[**] The authors acknowledge the financial support of a research grant from the MOE Program for Promoting Academic Excellence of Universities under grant No. 91-E-FA04-2-4-B and a JD research grant of Industry/Academia Cooperation Project provided by e-Ray Optoelectronics Technology Co., Ltd., who also provided many of the OLED materials used in this study.

 DOI: 10.1002/adma.200501169

ADVANCED MATERIALS

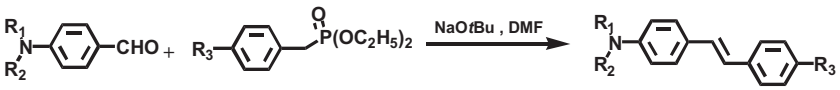

BD1 (R_1=R_2= Ph, R_3= 4-biphenyl)

BD2 (R_1= Ph, R_2= 2-napthyl, R_3= 4-biphenyl)

BD3 (R_1=R_2= *m*-tolyl, R_3= 4-biphenyl)

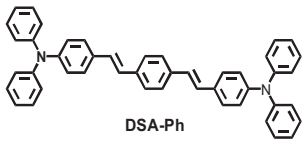

Scheme 1. Molecular structures of the deep-blue dopants used in this study. NaO*t*Bu = sodium *tert*-butoxide; DMF = dimethylformamide.

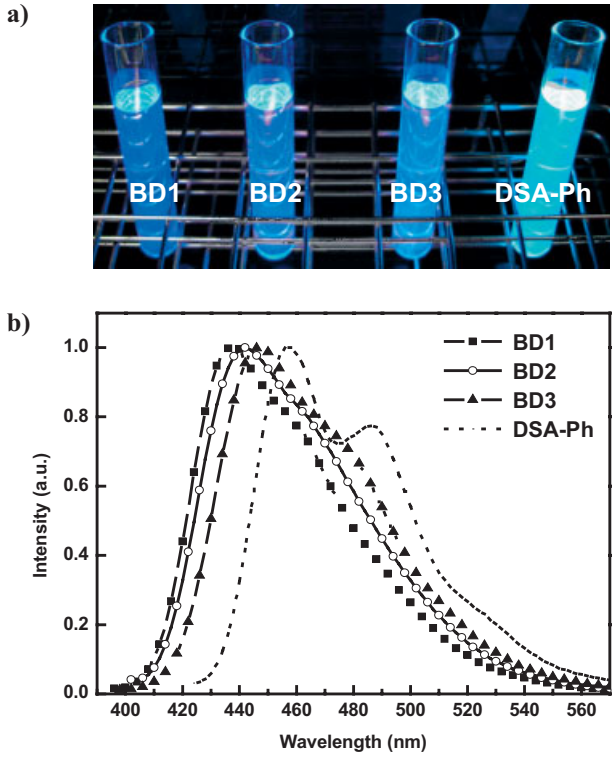

Figure 1. a) Solution photoluminscence of **BD1**, **BD2**, and **BD3** versus DSA-Ph in toluene. b) Their corresponding emission spectra.

To produce a deep-blue OLED in this study, the bluest dopant **BD1** has been chosen and MADN is used as the host. Three different blue device architectures were fabricated. For comparison purposes, device I has been designed as our standard blue device. Device II is a blue device with 10 nm of 2,9-dimethyl-4,7-diphenyl-1,10-phenanthroline (BCP) inserted between the emission layer (EML) and the electron-transport layer (ETL) as a hole-blocking layer (HBL). Device III is the blue device incorporating the novel c-HTL (40 nm). The detailed device architectures and molecular structures of MADN, NPB (*N*,*N*′-bis(1-naphtyl)-*N*,*N*′-diphenyl-1,1,1′-biphenyl-4,4′-diamine), tris(8-quinolinolato) aluminum (Alq_3), and BCP are shown in Figure 2, where CF_x is the hole-injection layer,[11] c-HTL and NPB together make up the hole-transport layer, **BD1**-doped MADN is the blue emitter, Alq_3 is the electron-transport layer, and Al/LiF is the bilayer cathode. In device III, c-HTL was deposited by the co-evaporation of copper pthalocyanine (CuPc) with NPB at the desired ratio (50:50). The purpose of inserting a thin layer of pure NPB in between c-HTL and EML (in device III) is to block electrons from reaching c-HTL. The lowest unoccupied molecular orbital (LUMO) of CuPc (~3.0 eV), which is lower than that of MADN (2.5 eV), has been shown to cause low luminance efficiency of the device due to non-radiative recombination in CuPc.[12]

The EL performance of device I, at an optimal doping concentration of 3 %, shows an EL efficiency of 2.2 cd A^{-1} at 20 mA cm^{-2} and 6.1 V, with an external quantum efficiency (EQE) of 2.3 %. The $CIE_{x,y}$ coordinates of device I lie in the saturated blue region at (0.15, 0.11). Figure 3 shows comparisons of luminance–current density–voltage (*B*–*I*–*V*) characteristics between devices I, II, and III. We discover that the EL efficiency of device II (driven at 20 mA cm^{-2}) can be significantly enhanced, by as much as 100 %, as compared to that of the standard device I. At an optimal concentration of 7 % doping, device II achieves an EL efficiency of 3.9 cd A^{-1} and 2.0 lm W^{-1} at 20 mA cm^{-2} and 6.2 V with $CIE_{x,y}$ coordinates of (0.15, 0.13). We attribute the dramatic increase in EL efficiency to the formation of a narrow recombination zone, in which both the charge carriers and the exciton are confined by the hole-blocking layer.[13] In addition, it is worth noting that in most other devices reported in the literature, when BCP is used as the HBL, the driving voltage is often considerably increased. This phenomenon has been rationalized by the poor electron mobility of BCP, which is known to be lower than that of Alq_3.[14] However, in our experiment, the *I*–*V* characteristics for both device I and II are essentially identical. We attribute this result to **BD1**, which possesses high hole-transporting mobility[15] and a low ionization energy potential (I_p = 5.2 eV) that is higher than those of NPB (I_p = 5.4 eV) and MADN (I_p = 5.6 eV). As a result, it provides a more effective pathway for hole injection directly from NPB to the dopant. Besides, the optimal **BD1** concentration of a BCP-based device is 7 %, which is much higher than that of a standard device (3 %). Thus, we believe that the high dopant concentration of **BD1** dispersed in the MADN host will further facilitate hole transport, which in turn will compensate for the low electron mobility of BCP in the device.

Another way to enhance the EL efficiency of the blue OLED is to further balance the hole and electron carriers arriving at the recombination zone, as the injected hole is usually more mobile than the injected electron under the same electric field in a conventional OLED. This is accomplished by inserting a novel c-HTL in the blue OLED (device III). A higher operating voltage was observed in this device with

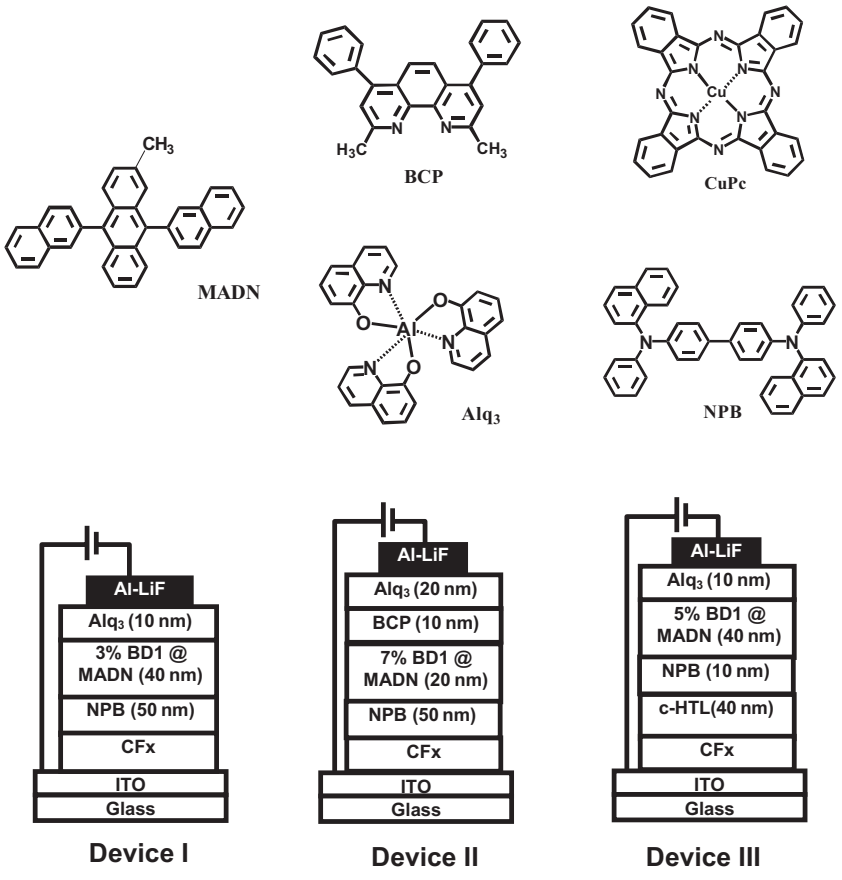

Figure 2. Molecular and device architectures used in this study. ITO is indium tin oxide; CF_x is the hole-injection layer; c-HTL and NPB together make up the hole-transport layer; **BD1**-doped MADN is the blue emitter; Alq_3 is the electron-transport layer; and Al/LiF is the bilayer cathode.

c-HTL, as compared to the standard device in Figure 3. This result is attributed to reduced hole transport by c-HTL, arising from two contributions: one is due to the "hole-impedance" of CuPc, and the other is owing to the dissipation of energy from the "trapping and de-trapping" mechanism of holes on the highest occupied molecular orbital (HOMO) of CuPc and NPB, since the ionization potential of CuPc ($I_p = 5.0$ eV) is much lower than that of NPB ($I_p = 5.4$ eV). More direct evidence of reduced hole transport by c-HTL can be observed from the *I–V* characteristics of the hole-only devices published in our previous work.[16] Consequently, the dramatic enhancement in luminance yield by incorporating c-HTL is believed to result from the slowing down of hole mobility, which in turn produces better carrier recombination at the emitting zone. As a result, at an optimal concentration of 5 % doping, device III achieves an EL efficiency of 5.4 cd A^{-1} and 2.5 lm W^{-1} at 20 mA cm^{-2} and 6.8 V, with $CIE_{x,y}$ coordinates of (0.14, 0.13). The overall EL performances of these blue devices, which are among the best ever reported in literature, are summarized in Table 1.

Figure 4 shows the operational lifetime ($t_{1/2}$) of these blue devices under a constant current density of 20 mA m^{-2} in a drybox. The initial luminance (L_0) measured for devices I, II, and III, was 440, 780, and 1080 cd m^{-2}, respectively. Assuming scalable coulombic degradation,[17] driving at an L_0 value of 100 cd m^{-2}, the half-lives ($t_{1/2}$) of devices I, II, and III are projected to be 10 000, 300, and 9700 h, respectively. We believe that the worst device operational lifetime of device II is primarily due to the intrinsic instability of the hole-blocking BCP material.[18] However, the device with c-HTL clearly demonstrates a more than double improvement in EL efficiency, as well as a comparable device operational lifetime to that of the standard device.

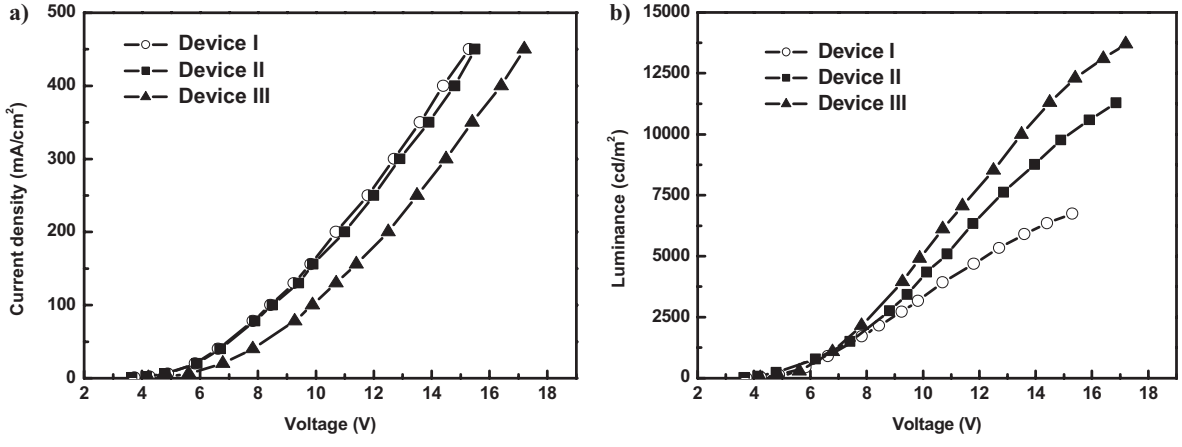

Figure 3. Comparison of a) *I–V* and b) *B–V* curves of **BD1**-doped devices I, II, and III.

ADVANCED MATERIALS

Table 1. EL performance of the three blue devices at 20 mA cm^{-2}.

Device	Luminance [cd m^{-2}]	Voltage [V]	1931 CIE		Luminance yield [cd A^{-1}]	Power efficiency [lm W^{-1}]	EQE [%]
			x	*y*			
I	440	6.1	0.15	0.11	2.2	1.5	2.3
II	780	6.1	0.15	0.13	3.9	2.0	3.6
III	1080	6.8	0.14	0.13	5.4	2.5	5.1

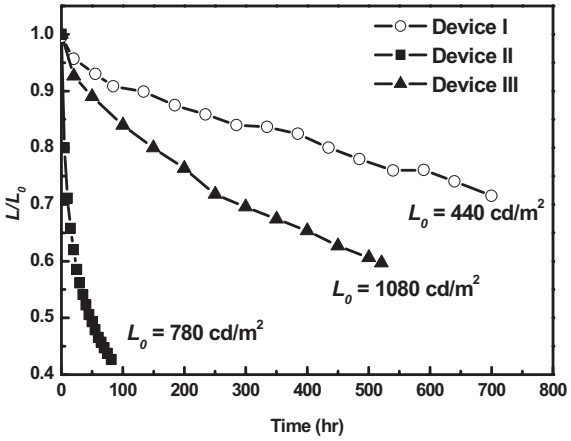

Figure 4. Operational lifetime tests for the blue devices used in this study.

In summary, carrier recombination as well as the balance of holes and electrons are considered to be some of the most important factors dictating the EQE of OLEDs. Here, we have developed a simple method to fabricate deep-blue OLEDs by introducing a novel c-HTL, which can effectively control the hole mobility to achieve an improved hole–electron balance. With this new device architecture and by employing our newly designed deep-blue dopant (**BD1**) with MADN as the host, we demonstrated one of the highest efficiencies (5.4 cd A^{-1}), color saturation (0.14, 0.13), and EQE (5.1 %) of deep-blue OLEDs ever reported in the literature. The operational lifetime for this device ($t_{1/2}$) is projected to be about 10 000 h at an initial luminance (L_0) of 100 cd m^{-2}.

Experimental

Synthesis: To a solution of 4-(*N*,*N*′-diarylamino)-benzoaldehyde (1 mmol) and phosphonate (1 mmol) in DMF placed in an ice bath, sodium *tert*-butoxide (1.5 mmol) was added. The solution was stirred at 25 °C for 1 h. The mixture was then poured into water, and the product was collected and washed with methanol. The products were purified by temperature gradient sublimation before use in subsequent studies.

Compound Characterization: **BD1**: ^{1}H NMR (300 MHz, $CDCl_3$): δ [ppm]: 7.57–7.70 (m, 10H), 7.36–7.49 (m, 5H), 7.25–7.30 (m, 5H), 7.01–7.14 (m, 10H). ^{13}C NMR (75 MHz, $CDCl_3$): δ [ppm]: 147.7, 147.6, 140.8, 140.2, 139.7, 139.6, 137.0, 131.7, 129.3, 128.8, 128.5, 127.5, 127.4, 127.3, 127.2, 127.1, 126.8, 126.7, 124.6, 123.7, 123.1. Fast atom bombardment mass spectroscopy (FAB MS): calcd molecular weight (MW): 499.7; *m/e* 500 [M$^+$]. Anal. for $C_{38}H_{29}N$: Calcd: C, 91.35; H, 5.85; N, 2.80. Found: C, 91.40; H, 6.13; N, 2.85.

BD2: ^{1}H NMR (300 MHz, $CDCl_3$): δ [ppm]: 7.57–7.79 (m, 12H), 7.26–7.49 (m, 12H), 7.03–7.18 (m, 6H). ^{13}C NMR (75 MHz, $CDCl_3$): δ [ppm]: 147.7, 147.5, 145.3, 140.8, 140.2, 139.7, 139.6, 136.9, 134.6, 132.0, 130.4, 129.4, 129.0, 128.8, 128.4, 127.6, 127.5, 127.5, 127.4, 127.2, 127.1, 126.9, 126.3, 124.8, 124.7, 124.6, 124.0, 123.4, 120.8. FAB MS: calcd MW: 549.7; *m/e* 549 [M$^+$]. Anal. for $C_{42}H_{31}N$: Calcd: C, 91.77; H, 5.68; N, 2.55. Found: C, 91.82; H, 5.86; N, 2.50.

BD3: ^{1}H NMR (300 MHz, $CDCl_3$): δ [ppm]: 7.58–7.70 (m, 9H), 7.44–7.54 (m, 3H), 7.23–7.39 (m, 4H), 7.09–7.18 (m, 3H), 6.85–7.04 (m, 7H), 2.35 (s, 3H), 2.28 (s,3H). ^{13}C NMR (75 MHz, $CDCl_3$): δ [ppm]: 147.7, 147.5, 147.3, 140.7, 140.1, 139.6, 139.4, 139.1, 137.1, 136.9, 130.4, 129.2, 129.0, 128.8, 127.9, 127.7, 129.5, 127.3, 127.2, 127.0, 126.8, 126.0, 125.2, 125.1, 124.3, 123.9, 122.7, 121.8, 121.6, 21.4, 20.1. FAB MS: calcd. MW: 527.7; *m/e* 528 [M$^+$]. Anal. for $C_{40}H_{33}N$: Calcd: C, 91.04; H, 6.30; N, 2.65. Found: C, 91.00; H, 6.45; N, 2.41.

UV-Vis and PL Characterization: The UV-vis absorption and photoluminescence spectra of these new dopants were measured in toluene using Hewlett Packard 8453 and Acton Research Spectra Pro-150 instruments, respectively.

OLED Fabrication: After a routine cleaning procedure of ultrasonication of the indium tin oxide (ITO)-coated glass in organic solvents and deionized water, followed by drying in an oven at 120 °C, the ITO substrate was loaded on the grounded electrode of a parallel-plate plasma reactor, pretreated with oxygen plasma, and then coated with a polymerized fluorocarbon film. Devices were fabricated under a base vacuum of about 10^{-6} torr (1 torr ≈ 133 Pa) in a thin-film evaporation coater, which followed a published protocol [17]. All devices were hermetically sealed prior to testing. The active area of the EL device, defined by the overlap of the ITO and the cathode electrodes, was 9 mm × 9 mm. The current–voltage–luminance characteristics of the devices were measured with a diode array rapid scan system using a Photo Research PR650 spectrophotometer and a computer-controlled, programmable, direct-current (DC) source.

Received: June 7, 2005
Published online: September 1, 2005

[1] C. W. Tang, S. A. Van Slyke, C. H. Chen, *J. Appl. Phys.* **1989**, *65*, 3610.

[2] a) Y. H. Kim, D. C. Shin, S. H. Kim, C. H. Ko, H. S. Yu, Y. D. Chae, S. K. Kwon, *Adv. Mater.* **2001**, *13*, 1690. b) J. Shi, C. W. Tang, *Appl. Phys. Lett.* **2002**, *80*, 3201. c) Y. Kan, L. Wang, L. Duan, Y. Hu, G. Wu, Y. Qiu, *Appl. Phys. Lett.* **2004**, *84*, 1513. d) M. T. Lee, Y. S. Wu, H. H. Chen, C. H. Liao, C. H. Tsai, C. H. Chen, in *Proc. of the Society for Information Display*, Society for Information Display, Santa Ana, CA **2004**, p. 710.

[3] C. Hosokawa, H. Higashi, H. Nakamura, T. Kusumoto, *Appl. Phys. Lett.* **1995**, *67*, 3853.

[4] C. C. Yeh, M. T. Lee, H. H. Chen, C. H. Chen, in *Proc. of the Society for Information Display*, Society for Information Display, Santa Ana, CA **2004**, p. 789.

[5] a) C. C. Wu, Y. T. Lin, K. T. Wong, R. T. Chen, Y. Y. Chien, *Adv. Mater.* **2004**, *16*, 61. b) T. C. Chao, Y. T. Lin, C. Y. Yang, T. S. Hung, H. C. Chou, C. C. Wu, K. T. Wong, *Adv. Mater.* **2005**, *17*, 992.

[6] a) L. H. Chan, H. C. Yeh, C. T. Chen, *Adv. Mater.* **2001**, *13*, 1637. b) J. U. Kim, H. B. Lee, J. S. Shin, Y. H. Kim, Y. K. Joe, H. Y. Oh, C. G. Park, S. K. Kwon, *Synth. Met.* **2005**, *150*, 27.

[7] a) A. Saitoh, N. Yamada, M. Yashima, K. Okinaka, A. Seno, K. Ueno, in *Proc. of the Society for Information Display*, Society for Information Display, Santa Ana, CA **2004**, p. 150. b) C. Hosokawa, K. Fukuoka, H. Kawamura, T. Sakai, M. Kubota, M. Funahashi, F. Moriwaki, H. Ikeda, *Proc. of the Society for Information Display*, Society for Information Display, Santa Ana, CA **2004**, p. 780. c) D. Gebeyehu, K. Walzer, G. He, M. Pfeiffer, K. Leo, J. Brandt, A. Gerhard, P. Stößel, H. Vestweber, *Synth. Met.* **2005**, *148*, 205.

[8] M. T. Lee, H. H. Chen, C. H. Liao, C. H. Tsai, C. H. Chen, *Appl. Phys. Lett.* **2004**, *85*, 3301.
[9] J. M. Kauffman, G. Moyna, *J. Org. Chem.* **2003**, *68*, 839.
[10] L. S. Hung, L. R. Zheng, M. G. Mason, *Appl. Phys. Lett.* **2001**, *78*, 673.
[11] M. H. Ho, Y. S. Wu, T. Y. Chu, J. F. Chen, C. H. Chen, in *Proc. of the Int. Display Manufacturing Conf.*, Society for Information Display, Santa Ana, CA **2005**, p. 726.
[12] C. H. Liao, C. H. Tsai, C. H. Chen, in *Proc. of the 24th Int. Display Research Conf./4th Int. Meeting on Information Display*, Society for Information Display, Santa Ana, CA **2004**, p. 724.
[13] Z. Y. Xie, L. S. Hung, S. T. Lee, *Appl. Phys. Lett.* **2001**, *79*, 1048.
[14] a) Y. Li, M. K. Fung, Z. Xie, S. T. Lee, L. S. Hung, J. Shi, *Adv. Mater.* **2002**, *14*, 1317. b) Z. Wu, H. Yang, Y. Duan, W. Xie, S. Liu, Y. Zhao, *Semicond. Sci. Technol.* **2003**, *18*, L49.
[15] H. Ueda, T. Kitahora, K. Furukawa, Y. Tersaka, *Synth. Met.* **1997**, *91*, 257.
[16] C. H. Liao, M. T. Lee, C. H. Tsai, C. H. Chen, *Appl. Phys. Lett.* **2005**, *86*, 203 507.
[17] S. A. Van Slyke, C. H. Chen, C. W. Tang, *Appl. Phys. Lett.* **1996**, *69*, 2160.
[18] Y. Kim, W. B. Im, *Phys. Status Solidi A* **2004**, *201*, 2148.

The Zwitterion Effect in Ionic Liquids: Towards Practical Rechargeable Lithium-Metal Batteries**

By *Nolene Byrne*, *Patrick C. Howlett*, *Douglas R. MacFarlane*, and *Maria Forsyth**

The quest for the development of rechargeable lithium-metal batteries has attracted vigorous worldwide research efforts. The advantage of lithium-metal-based batteries over traditional nickel–cadmium, nickel-metal-hydride, and lithium-ion batteries is the higher theoretical energy density of metallic lithium.[1] The key limitation of the lithium-metal battery is the growth of dendrites during cycling.[2] This is potentially hazardous and leads to reduced cycle lifetime. A number of well-documented accidents have occurred with experimental cells due to this problem, and as a result research had largely stopped until recently.[3] Hence, to realize the ultimate potential of the lithium-metal cell, a means to suppress dendrite growth is required.

[*] Prof. M. Forsyth, N. Byrne, Dr. P. C. Howlett
ARC Centre of Nanostructured Electromaterials
School of Physics and Materials Engineering, Monash University
Wellington Rd, Clayton, Victoria 3800 (Australia)
E-mail: maria.forsyth@spme.monash.edu.au
Prof. D. R. MacFarlane
ARC centre of Nanostructured Electromaterials,
School of Chemistry, Monash University
Wellington Rd, Clayton, Victoria 3800 (Australia)

[**] The authors acknowledge financial support from the ARC through the Centre of Nanostructured Electromaterials. We also thank Anita Hill and Anthony Hollenkamp for insightful discussion.

Alternative electrolytes have been investigated, such as the use of a solid electrolyte to act as a mechanical barrier,[1] or electrolytes which control the properties of the solid-electrolyte interphase (SEI), i.e., the passivation layer, which is now well accepted as forming on the lithium-metal surface.[4] The SEI layer controls the performance of the battery by protecting the lithium-metal surface, while still allowing Li-ion transport. At the extremely negative potential of the lithium electrode the presence of an SEI appears to be ubiquitous.[5] It is also well known that the composition and morphology of the SEI layer can be controlled through the use of additives, which can improve plating behavior and cycle lifetime.[6] Nonetheless, the limited cycle life and safety problems associated with dendrite formation remain in devices incorporating these volatile electrolytes.

It has recently been shown by Howlett et al., Passerini and co-workers, Katayama et al., and Sakaebe et al.[7] that a new class of electrolytes—room-temperature ionic liquids (RTILs)—have properties that can support lithium electrochemistry. In addition, ionic-liquid electrolytes facilitate enhanced cycling efficiency and favorable plating morphology of lithium.[7a] These electrolytes, in particular the *N*-methyl-*N*-alkylpyrrolidinium bis(trifluoromethanesulfonyl)amide[8] family of ionic liquids, are finding wide use in many electrochemical devices, such as electrochromic windows,[9] dye-sensitized solar cells,[10] and other devices.[9] Ionic liquids have many properties which make them highly suitable for use in rechargeable lithium batteries: these properties include excellent thermal stability, effectively zero volatility and flammability, high conductivity, and a wide electrochemical window. Nevertheless, despite improved cycling performance when compared to most traditional solvent-based electrolytes, dendrite formation still occurs when practical current densities are used.[7a] This dendrite formation may be due to mass-transport limitations either in the electrolyte, or in the SEI layer itself. Ultimately this is what restricts the application of ionic-liquid electrolytes in rechargeable lithium-metal and lithium-ion batteries.

Zwitterionic compounds (Scheme 1) are compounds that are designed to tether the anion and cation making up the above-mentioned ionic liquids, preventing migration under the influence of an electric field. These compounds were first pioneered by Ohno and co-workers[11] and, since then, we have shown that the use of these zwitterionic compounds largely enhance lithium-ion diffusivity in polyelectrolyte gels.[12] The mechanism by which the zwitterions enhance lithium-ion transport is not yet clear; it has been suggested that it may occur by shielding ion–ion interactions and hence increasing dissociation. Alternatively, the zwitterions may

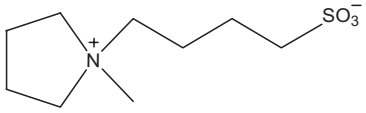

Scheme 1. *N*-methyl-*N*-(butyl sulfonate) pyrrolidinium.

 DOI: 10.1002/adma.200500595